Article

(*n*,*m*) Selectivity of Single-Walled Carbon Nanotubes by Different Carbon Precursors on Co–Mo Catalysts

Bo Wang, C. H. Patrick Poa, Li Wei, Lain-Jong Li, Yanhui Yang, and Yuan Chen

J. Am. Chem. Soc., **2007**, 129 (29), 9014-9019• DOI: 10.1021/ja070808k • Publication Date (Web): 30 June 2007

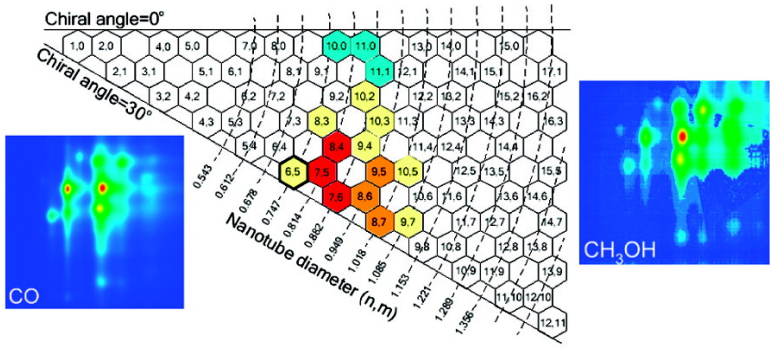

More About This Article

Additional resources and features associated with this article are available within the HTML version:

- Supporting Information
- Links to the 14 articles that cite this article, as of the time of this article download
- Access to high resolution figures
- Links to articles and content related to this article
- Copyright permission to reproduce figures and/or text from this article

View the Full Text HTML

J|A|C|S
ARTICLES
Published on Web 06/30/2007

(*n,m*) Selectivity of Single-Walled Carbon Nanotubes by Different Carbon Precursors on Co−Mo Catalysts

Bo Wang,[§] C. H. Patrick Poa,[†] Li Wei,[§] Lain-Jong Li,[‡] Yanhui Yang,[§] and Yuan Chen*,[§]

Contribution from the School of Chemical and Biomedical Engineering, Nanyang Technological University, Singapore 637459, Institute of Materials Research and Engineering, Singapore 117602, and School of Materials Science and Engineering, Nanyang Technological University, Singapore 639798

Received February 4, 2007; E-mail: chenyuan@ntu.edu.sg

Abstract: Single walled carbon nanotubes (SWCNTs) were synthesized using four different carbon precursors including CO, C_2H_5OH, CH_3OH, and C_2H_2 on Co−Mo catalysts. Semiconducting (*n,m*) abundance was evaluated by a method based on a single-particle tight-binding theoretical model taking into consideration the relative photoluminescence and absorption quantum efficiency for specific (*n,m*) tubes. (*n,m*) abundance determined in photoluminescence analysis was used to reconstruct the near-infrared E^s_{11} absorption spectra. Carbon precursor pressure was found to be the key factor to the chirality control in this study. Narrowly (*n,m*) distributed SWCNTs can only be obtained under high-pressure CO or vacuumed C_2H_5OH and CH_3-OH. The majority of these nanotubes are predominately in the same higher chiral-angle region. The carbon precursor chemistry may also play an important role to obtain narrowly (*n,m*) distributed SWCNTs. (*n,m*) selectivity on Co−Mo catalysts shifts under different carbon precursors providing the route for (*n,m*) specific SWCNTs production.

Introduction

Single-walled carbon nanotubes (SWCNTs) are widely recognized as potential building blocks for future nanoscale electronics.[1] Their electronic properties strongly depend on their diameter and chiral angle, which are identified as the chiral indices (*n,m*). One of the major obstacles to applications of SWCNTs in nanoscale electronics is the control of the synthesis processes to produce SWCNTs with desired (*n,m*) structure. Most synthesis methods result in a wide distribution of (*n,m*) species.[2,3] The obstacles exist on two aspects: (1) accurately characterizing (*n,m*) SWCNT abundance in a given sample; (2) understanding the mechanism of chirality selectivity under different growth conditions.

Photoluminescence (PL) and tunable-laser excitation resonance Raman spectroscopy (RRS) can be applied for the assignment of the majority of (*n,m*) SWCNTs.[4,5] Recent studies indicate that one theoretical model[6] (based on the single-particle tight-binding theory), providing good analytical predictions about the relative PL quantum efficiency and absorption extinction coefficients of various (*n,m*) SWCNTs, could be applied to evaluate abundance profiles for all semiconducting (*n,m*) SWCNTs for a given sample.[7] Narrow (*n,m*) distribution SWCNTs have been grown on Co−Mo catalysts[8] and Co−MCM-41[9−11] using CO as well as an ethanol growth process.[12] An intriguing phenomenon is that these narrow (*n,m*) distribution SWCNTs are predominant in the same higher chiral-angle region. Theoretical study proposed that particular chirality could be favored by the epitaxial relationship between the nanotube cap and the solid catalyst surface.[13] Our intention is to alter the chirality selectivity by different carbon precursors, which have distinct decomposition rate and chemical composition. If the

§ School of Chemical and Biomedical Engineering, Nanyang Technological University.
† Institute of Materials Research and Engineering.
‡ School of Materials Science and Engineering, Nanyang Technological University.

(1) Dresselhaus, M. S., Dresselhaus, G., Avouris, P., Eds. *Carbon Nanotubes Synthesis, Structure, Properties, and Applications*. Topics in Applied Physics; 2001; Vol. 80, p 447.
(2) Henrard, L.; Loiseau, A.; Journet, C.; Bernier, P. *Synth. Met.* **1999**, *103* (1−3), 2533−2536.
(3) Nikolaev, P.; Bronikowski, M. J.; Bradley, R. K.; Rohmund, F.; Colbert, D. T.; Smith, K. A.; Smalley, R. E. *Chemi. Phys. Lett.* **1999**, *313* (1,2), 91−97.
(4) Bachilo, S. M.; Strano, M. S.; Kittrell, C.; Hauge, R. H.; Smalley, R. E.; Weisman, R. B. *Science* **2002**, *298* (5602), 2361−2366.
(5) O'Connell, M. J.; Bachilo, S. M.; Huffman, C. B.; Moore, V. C.; Strano, M. S.; Haroz, E. H.; Rialon, K. L.; Boul, P. J.; Noon, W. H.; Kittrell, C.; Ma, J. P.; Hauge, R. H.; Weisman, R. B.; Smalley, R. E. *Science* **2002**, *297* (5581), 593−596.
(6) Oyama, Y.; Saito, R.; Sato, K.; Jiang, J.; Samsonidze, G. G.; Gruneis, A.; Miyauchi, Y.; Maruyama, S.; Jorio, A.; Dresselhaus, G.; Dresselhaus, M. S. *Carbon* **2006**, *44* (5), 873−879.
(7) Luo, Z. T.; Pfefferle, L. D.; Haller, G. L.; Papadimitrakopoulos, F. *J. Am. Chem. Soc.* **2006**, *128* (48), 15511−15516.
(8) Bachilo, S. M.; Balzano, L.; Herrera, J. E.; Pompeo, F.; Resasco, D. E.; Weisman, R. B. *J. Am. Chem. Soc.* **2003**, *125* (37), 11186−11187.
(9) Ciuparu, D.; Chen, Y.; Lim, S.; Haller, G. L.; Pfefferle, L. *J. Phys. Chem. B* **2004**, *108* (2), 503−507.
(10) Chen, Y.; Ciuparu, D.; Lim, S.; Yang, Y. H.; Haller, G. L.; Pfefferle, L. *J. Catal.* **2004**, *226* (2), 351−362.
(11) Chen, Y.; Ciuparu, D.; Lim, S. Y.; Yang, Y. H.; Haller, G. L.; Pfefferle, L. *J. Catal.* **2004**, *225* (2), 453−465.
(12) Miyauchi, Y.; Chiashi, S.; Murakami, Y.; Hayashida, Y.; Maruyama, S. *Chem. Phys. Lett.* **2004**, *387* (1−3), 198−203.
(13) Reich, S.; Li, L.; Robertson, J. *Chem. Phys. Lett.* **2006**, *421* (4−6), 469−472.

10.1021/ja070808k CCC: $37.00

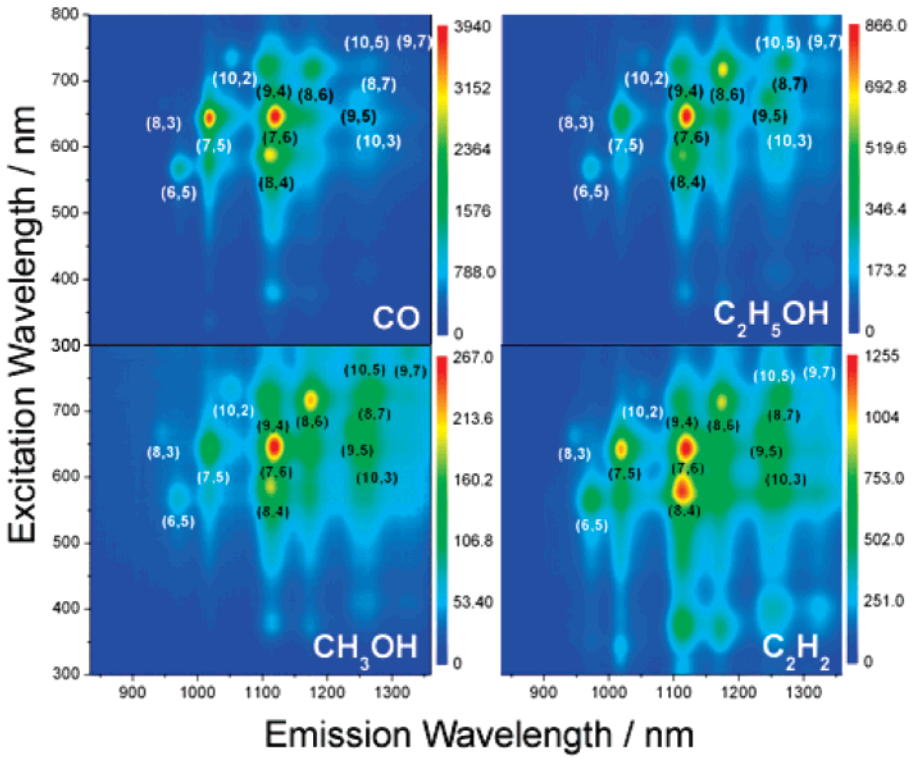

Figure 1. Photoluminescence excitation (PLE) intensity map as a function of excitation and emission wavelength for SDBS micellarized SWCNTs in D_2O produced from four different carbon precursors on Co−Mo catalysts.

narrow chirality selectivity is kinetically controlled, we should be able to obtain SWCNTs with distinct and narrow (*n*,*m*) distribution.

In this study, we utilized fluorescence spectroscopy and absorption spectroscopy to analyze the abundance of different semiconducting (*n*,*m*)-SWCNTs on four representative samples synthesized from CO, C_2H_5OH, CH_3OH, and C_2H_2 carbon precursors. It was found that by carefully adjusting the pressure on these precursors, narrowly (*n*,*m*) distributed SWCNTs can be obtained from CO, C_2H_5OH, and CH_3OH, and the majority of these nanotubes are predominately in the same higher chiral-angle region. (*n*,*m*) selectivity shifts among different precursors.

Experimental Section

The silica (Sigma-Aldrich SiO_2 with 6 nm average pore size and Brunauer−Emmett−Teller (BET) surface area of 480 $m^2\ g^{-1}$) supported Co−Mo catalysts (4.6 wt % Mo, at a 1:3 Co/Mo molar ratio) were prepared by incipient wetness impregnation of an aqueous solution of cobalt nitrate and ammonium heptamolybdate. An amount of 0.54 g $Co(NO_3)_2{\cdot}6H_2O$ (Sigma-Aldrich 99.999%) and 0.98 g $(NH_4)_6Mo_7O_{24}{\cdot}4H_2O$ (Sigma-Aldrich, 99.98%) were dissolved in 20 mL DI water separately and slightly stirred for 10 min. These two solutions then were mixed together and stirred for another 10 min. Silica gel (10 g) was slowly added to the solution in 20 min with continued stirring at room temperature. The impregnated material was then dried at 105 °C for 12 h and then calcined at 500 °C for 3 h. In a typical SWCNT growth experiment, 400 mg of calcined Co−Mo catalysts were prereduced under 1 bar flowing H_2 (80 sccm) using a temperature ramp of 10 °C/min to 500 °C. Once the temperature reached 500 °C, the reactor was purged using flowing Ar (250 sccm), while the temperature was further increased to 800 °C. For the pressured carbon precursor (CO, the carbonyls were eliminated by Nanochem Purifilter by Matheson Gas Products), CO flow of 50 sccm was introduced into the reactor at 6 bar and kept for 30 min. For C_2H_5OH and CH_3OH, narrow (*n*,*m*) distribution SWCNTs were only obtained under vacuum conditions. Once 800 °C was reached, the reactor was evacuated by a rotary pump to 5 mbar. C_2H_5OH or CH_3OH vapor from a reservoir, where the temperature was maintained at 30 and 0 °C, respectively, was introduced for 30 min at a constant total pressure of 5 mbar. Owing to its extremely fast decomposition rate, C_2H_2 was further diluted in Argon at 1:1000 ratio before being introduced into the reactor at 5 mbar and total flow rate of 500 sccm. Three runs for each carbon source under identical conditions were tested to validate the run-to-run fluctuation versus differences among runs using different carbon sources. The synthesized SWCNTs were refluxed in 1.5 mol/L NaOH solution to dissolve the silica supports and filtered by Nylon membrane with 0.22 μm pore size to remove silica dissolved in NaOH. The purified SWCNTs were suspended in 1% sodium dodecyl benzene sulfonate SDBS/D_2O (99.9 atom % D, Sigma-Aldrich) solution and sonicated using a cup−horn ultrasonicator (SONICS, VCX-130) at 20 W for 30 min. After ultrasonication, the suspension was centrifuged for 1 h at ca. 53000g to remove the catalyst particles and other carbon impurities. Fluorescence spectroscopy measurements were conducted on a Jobin-Yvon Nanolog-3 spectrofluorometer equipped with an IGA (InGaAs) near-infrared (NIR) detector. The UV−vis−NIR absorption spectra were measured on a Varian Cary 5000 UV−vis−NIR spectrophotometer.

Results and Discussion

Figure 1 illustrates the two-dimensional PL excitation map for the aqueous dispersion of SWCNTs produced by four carbon precursors with excitation scanned from 300 to 800 nm and emission collected from 830 to 1360 nm. The resonance behavior of both excitation and emission events results in spikes corresponds to the transition pair from individual (*n*,*m*) SWCNTs.[4] Figure 1 suggests that narrowly (*n*,*m*) distributed SWCNTs were produced using four different carbon precursors. The chirality map for SWCNT samples in Figure 2 shows that (*n*,*m*) distributions are predominantly in the same higher chiral-angle region originating from (7,5), (7,6), (8,4), and (8,6). The strength

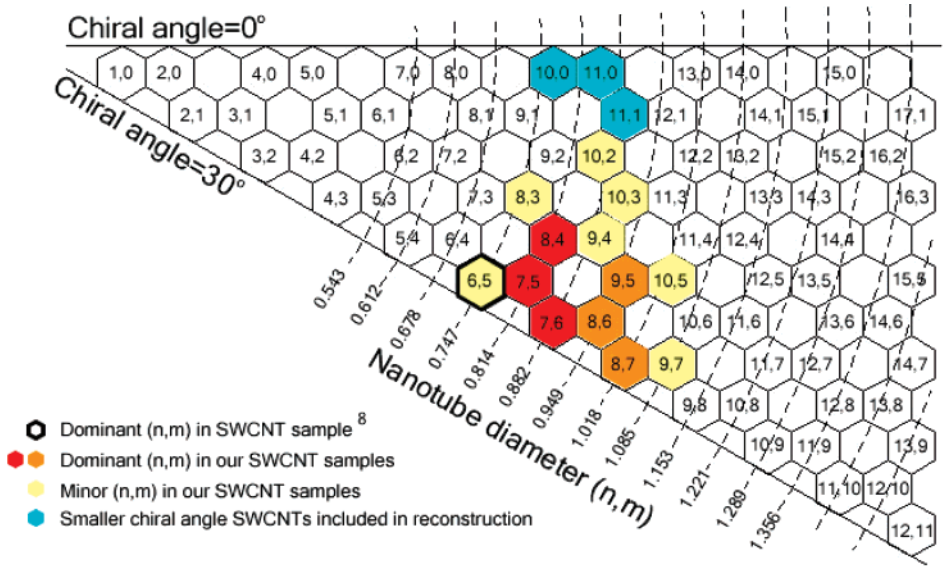

Figure 2. Chirality maps of SWCNT samples produced from three different carbon precursors: CO, C_2H_5OH, and CH_3OH. Red and orange hexagons are dominant (*n*,*m*) species produced, yellow hexagons are other minor (*n*,*m*) species identified in PL analysis. Blue hexagons are those included in absorption spectra reconstruction as discussed later. (*6*,*5*) were dominant tubes from Bachilo et al.[8]

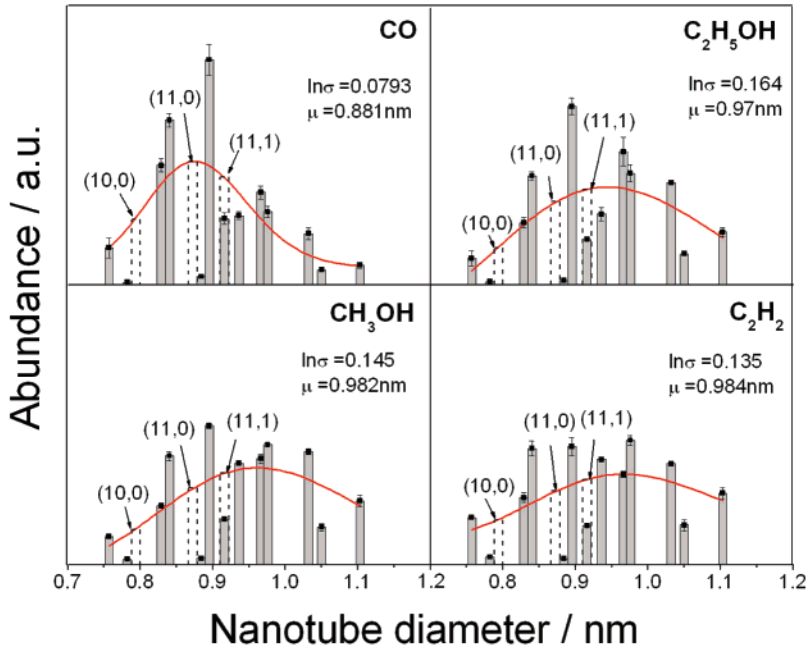

Figure 3. Calculated diameter distribution histograms (bars) obtained in PL analysis and their log-normal fits. Dashed bars in panel indicate the possible position of the (10,0) and (11,0) zigzag SWCNTs and (11,1) small chiral-angle tubes.

of the (*n*,*m*) chirality from PL map was determined from the amplitude of the partial derivative, as recommended by Arnold et al.[14] to minimize the effects of the slowly varying background. CO produced the narrowest (*n*,*m*) distribution dominated at (7,6), (7,5), and (8,4). C_2H_5OH and CH_3OH produced more (8,6), (9,5), and (8,7) as shown in Figure 2 and Table S1, Supporting Information.

Taking into consideration of the relative PL quantum efficiency of various (*n*,*m*) SWCNTs, using the methodology developed by Luo et al.[7] based on a single-particle electron−phonon interaction model,[6] the abundance of a particular (*n*,*m*) SWCNT was listed in Table S1, Supporting Information. To validate the run-to-run fluctuation versus differences among runs using different carbon sources, three parallel runs for each carbon source under identical conditions were tested. Figure S1, Supporting Information, indicates that (*n*,*m*) distribution changes are caused by different carbon precursors and the run-to-run fluctuation is in a reasonable range. Figure 3 illustrates the histograms of diameter distribution of SWCNTs that were extracted from Figure S1 and Table S1. The error bars in Figure 3 show the run-to-run fluctuation of three parallel experiments.

As PL intensity of different (*n*,*m*) SWCNTs could be altered by the effects of different surfactants, sonication-induced changes, and nanotube lengths on the quantum yields,[15] a series

(14) Arnold, M. S.; Green, A. A.; Hulvat, J. F.; Stupp, S. I.; Hersam, M. C. *Nat. Nanotechnol.* **2006**, *1* (1), 60−65.

(15) Heller, D. A.; Mayrhofer, R. M.; Baik, S.; Grinkova, Y. V.; Usrey, M. L.; Strano, M. S. *J. Am. Chem. Soc.* **2004**, *126* (44), 14567−14573.

of controlled experiments using four different surfactants for various sonication durations were performed. Although the PL intensity can be different because of the SWCNT concentration in solution, the (*n*,*m*) abundance distribution is not affected as shown in Figure S2.

We need to emphasize that two issues may complicate the accuracy of a particular (*n*,*m*) SWCNT abundance determined from PL experimental results. (1) Experimental results[4,5,12,16,17] have shown that the relative PL intensity of the zigzag and small chiral-angle semiconducting SWCNTs is significantly lower than that from large chiral-angle tubes at the same tube-diameter range. The absence of the PL signal from zigzag tubes (10,0), (11,0) and small chiral-angle tube (11,1) in our samples may be due to their low PL quantum efficiency.[6] (2) The large diameter nanotubes also have relatively lower PL intensity than that of smaller diameter nanotubes as pointed out by researchers.[18−22] Especially, for SWCNTs produced by C_2H_2, some larger diameter nanotubes may not be detected by PL analysis.

To reconcile our findings, we adopted the methodology developed by Luo et al.[7] to reconstruct the NIR absorption manifold of the E^S_{11} transition. The overall contribution to the expected optical density (OD) of all (*n*,*m*) SWCNTs at a specific optical energy *E* can be calculated by using the following equation, where *C* is the normalization factor introduced to account for sampling conditions and the collection geometries. $I^{abs}_{cal}(n,m)$ values for E^S_{11} transitions were taken from the calculated E^S_{22} extinction coefficients for the single-particle tight-binding theoretical model. $E_{11}(n,m)$ values were obtained from PL measurements of Figure 1 and γ_e is the width of the optical transitions, which is related to the lifetime of the excited states; we approximated $\gamma_e = C_1 + C_2/I^{abs}_{cal}(n,m)$ with C_1 and C_2 as adjustable parameters.

$$\mathrm{OD}(E) = C \sum_{n,m} A(d_t) I^{abs}_{cal}(n,m) \frac{\gamma_e}{4(E - E_{11}(n,m))^2 + {\gamma_e}^2} \qquad (1)$$

A single-mode log-normal distribution line shape[7] was applied to fit the experimental data as shown in Figure 3. The log-normal diameter distribution function for the CO produced sample, $A(d_t)$ obtained in Figure 3a for all (*n*,*m*) tubes, was first utilized in reconstruction. For one extreme case, where we assumed no diameter-induced chirality is imparted by the catalyst, zigzag (10,0) and (11,0) and small chiral-angle tube (11,1) were introduced. The other extreme case corresponds to the complete absence of these small chiral-angle tubes. However, as shown in Figure S3, Supporting Information, the reconstruction of the E^S_{11} for both cases is unsuccessful. We noticed that the (*n*,*m*) abundance determined by PL analysis in our sample is quite apart from the proposed single-mode log-normal distribution compared with the sample studied by Luo et al.[7] One scenario might be that the chiral selective growth is at play. Particular chirality could be favored in CVD growth. To verify this, we applied a three-steps fitting strategy. First, we directly used the $A(d_t)$ determined by PL analysis (Table S1a) to reconstruct the NIR absorption spectrum. The fitting result shown in Figure 4b is significantly improved compared with those in Figure S3. Second, we added in the two zigzag tubes and one small chiral-angle tube using their abundance obtained by the log-normal

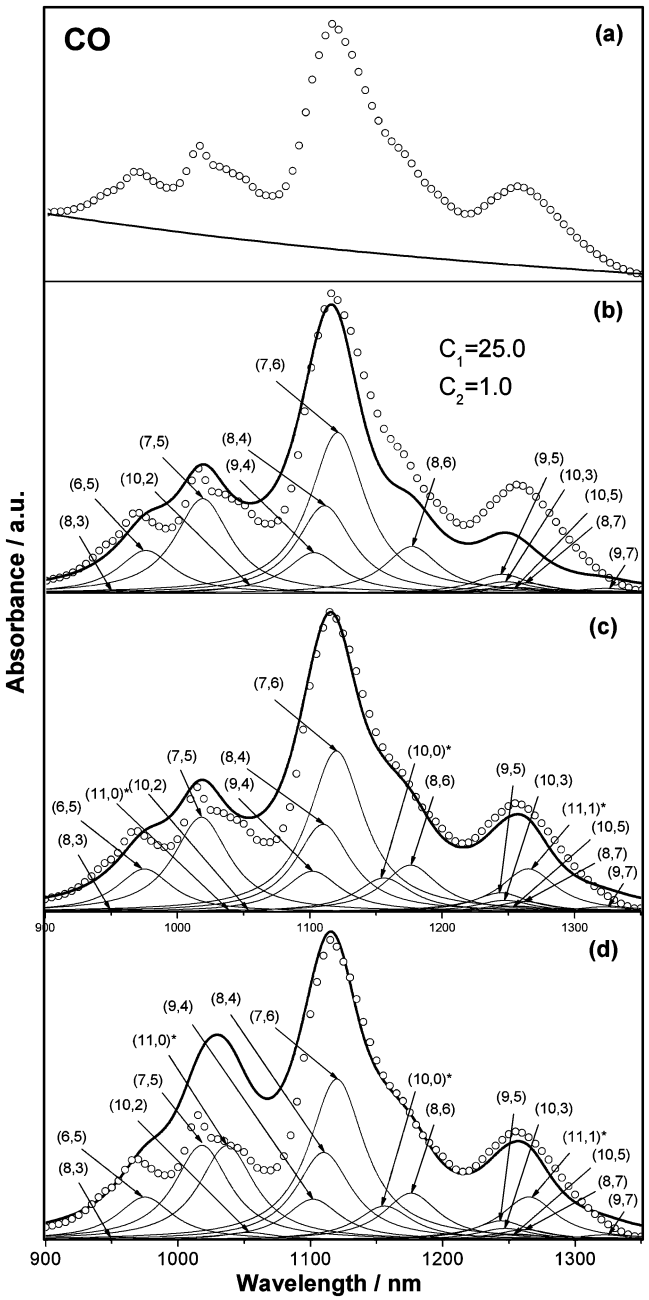

Figure 4. (a) Experimental E^S_{11} optical absorption spectrum (circles) and background curve (solid line) of aqueous SDBS dispersed SWCNTs suspensions grown by CO. The spectra indicated with circles in panels b, c, and d were obtained by subtracting the two curves in panel a. (b) Spectral reconstruction by the summation of the thin Lorentzian peak contribution from each (*n*,*m*) SWCNTs using the abundance determined by PL analysis without (10,0), (11,0), and (11,1) nanotubes. (c) Reconstruction by adding (10,0), (11,0), and (11,1 whose abundances are approximately at the average level of minor tubes identified in Figure 2. (d) Reconstruction adding (10,0), (11,0), and (11,1) nanotubes, whose abundances are determined by the log-normal diameter distribution.

(16) Strano, M. S. *J. Am. Chem. Soc.* **2003**, *125* (51), 16148−16153.
(17) Strano, M. S.; Zheng, M.; Jagota, A.; Onoa, G. B.; Heller, D. A.; Barone, P. W.; Usrey, M. L. *Nano Lett.* **2004**, *4* (4), 543−550.
(18) Fantini, C.; Jorio, A.; Souza, M.; Strano, M. S.; Dresselhaus, M. S.; Pimenta, M. A. *Phys. Rev. Lett.* **2004**, *93* (14), 147406/1−147406/4.
(19) Telg, H.; Maultzsch, J.; Reich, S.; Hennrich, F.; Thomsen, C. *Phys. Rev. Lett.* **2004**, *93* (17), 177401/1−177401/4.
(20) Jorio, A.; Fantini, C.; Pimenta, M. A.; Capaz, R. B.; Samsonidze, G. G.; Dresselhaus, G.; Dresselhaus, M. S.; Jiang, J.; Kobayashi, N.; Gruneis, A.; Saito, R. *Phys. Rev. B* **2005**, *71* (7).
(21) Goupalov, S. V.; Satishkumar, B. C.; Doorn, S. K.*Phys. Rev. B* **2006**, 73 (11).
(22) Lim, Y. S.; Yee, K. J.; Kim, J. H.; Haroz, E. H.; Shaver, J.; Kono, J.; Doorn, S. K.; Hauge, R. H.; Smalley, R. E. *Nano Lett.* **2006**, *6* (12), 2696−2700.

diameter distribution from Figure 3a. The result in Figure 4d shows that part of the reconstruction result (>1100 nm) is improved, while the other part (<1100 nm) gets worse. Third, we included the (10,0), (11,0) and (11,1) tubes; however, their abundance was set approximately at the average abundance level of those minor tubes identified in Figure 2. An improved reconstruction was obtained as shown in Figure 4c. Based on intensity variation between the experimental and reconstructed spectra in Figure S3 and 4, we conclude that the sample produced by CO in our study has the composition close to the abundance distribution obtained by PL analysis. Zigzag tubes present at lower concentrations compared with higher chiral-angle tubes. The main (*n*,*m*) species are predominately in the higher chiral-angle region.

Similar analysis routines were conducted for samples produced from C_2H_5OH, CH_3OH, and C_2H_2. As in the same case as that of CO, if we adopt the abundance of a specific (*n*,*m*) tube obtained by the single-mode log-normal distribution line shape, no matter whether we include the zigzag tubes or not, reconstruction of the E^S_{11} absorption spectra is unsuccessful. The results are shown in Figure S4, S5, and S6 for C_2H_5OH, CH_3OH, and C_2H_2, respectively. On the other hand, if $A(d_t)$ determined by PL analysis was utilized for SWCNT samples produced by C_2H_5OH and CH_3OH, the reconstruction of NIR E^S_{11} absorbance spectra can be achieved as shown in Figure S7 and S8, respectively. There are mismatches of experiential and reconstructed spectra between 900 and 1000 nm, especially for CH_3OH (Figure S8). We suspect that it may due to the overlap of E^S_{22} bands from some larger diameter tubes and E^S_{11} bands of smaller diameter tubes. Even so, based on the intensity in absorption spectra, abundance of larger diameter tubes should be low compared with dominant (*n*,*m*) tubes. We conclude that the samples produced by C_2H_5OH and CH_3OH also have the (*n*,*m*) abundance distribution similar to that obtained by PL analysis. The main (*n*,*m*) species are predominately in the higher chiral-angle region.

However, the reconstruction of C_2H_2 spectra cannot be achieved as shown in Figure S6 and S9. These results suggest that large diameter nanotubes having relative lower PL intensity constitute a significant fraction of SWCNTs produced by C_2H_2. Much broader (*n*,*m*) distribution is obtained in the SWCNT samples.

We found that the pressure of the carbon precursor is a key factor to the chirality control in this study. Only at high CO pressure were narrow (*n*,*m*) distribution SWCNTs obtained. Amorphous carbon was produced under vacuumed CO. On the contrary, C_2H_5OH and CH_3OH only grew SWCNTs under vacuum conditions. C_2H_2 needed to be further diluted by 1000 times in Ar at 5 mbar, otherwise no SWCNTs were produced, and even so narrowly (*n*,*m*) distributed SWCNTs have not been obtained. Lu et al.[23] have proposed the hypothesis that the diameters of SWCNTs were closely related to the carbon feeding rate by selective activation of nanoparticles. We reason that the pressure determines the striking frequency of a carbon precursor on the cobalt cluster surfaces. Meanwhile these four different carbon precursors would have different decomposition rates on the cobalt surface at 800 °C; for example, C_2H_2 decomposes much faster than CO. The carbon feeding rate to cobalt surfaces is then tuned by pressure, leading to different (*n*,*m*) selectivity.

The narrow (*n*,*m*) selectivity of Co−Mo catalyst has been attributed to small Co clusters formed in-situ and stabilized by Mo carbide.[8] Lolli et al.[24] have found that different (*n*,*m*) distributions were produced by using CO and CH_4. Although their abundance analysis did not consider the absorption extinction coefficients, absorption spectra of SWCNTs produced by CH_4 did indicate much wider (*n*,*m*) distribution compared with that by CO, due to the different kinetic behavior of CH_4 decomposition. They argued that kinetic effect rather than thermodynamic effect should be considered toward the chirality control. The results in this study show that narrow (*n*,*m*) selectivity on Co−Mo can be shifted using different carbon precursors. The dominant (*n*,*m*) species produced by CO in this research is about 0.1 nm larger in diameter compared with previous results,[8] probably owing to the different catalyst prereduction condition and CO pressure applied. The spread of (*n*,*m*) distribution produced in this study is at the similar level compared with Bachilo et al.,[8] while much narrower compared with HiPco nanotubes. Moreover, C_2H_5OH and CH_3OH increased the diameter of dominant (*n*,*m*) species by 0.05−0.2 nm (Figure 2). Because the cobalt clusters were continuously agglomerating owing to high-temperature sintering during the SWCNT growth, we argue that other than one (*n*,*m*) tube with global minimum stability energy (e.g., (7,6)) on metal cluster surfaces, several local minimum could coexist with a small difference in stability. When different carbon feeding rates match with these local minimum stabilities, SWCNTs enriched with various (*n*,*m*) can be produced. By fine-tuning the growth conditions, the controlled production of specific (*n*,*m*) structures could be achieved. Further studies are in progress.

In addition to the pressure effect, the carbon precursor chemistry may also play an important role for attaining narrow diameter distribution nanotubes. Lolli et al.[24] have discussed the difference between CO and CH_4 and attribute the broader distribution of SWCNTs produced by CH_4 to the evolution of hydrogen, a byproduct of the CH_4 decomposition. Hydrogen not only may increase the rate of reduction and sintering of metal clusters but also may hinder the nucleation of carbon species on the surface of the cluster by decreasing the carbon surface fugacity.[24] Zhang et al.[25] also pointed out that hydrogen radicals are damaging the formation of sp^2-like SWCNTs in plasma enhanced CVD and showed that the addition of oxygen in the carbon precursors scavenges the H species, providing an environment which favors SWCNT growth. We reason that the broader distribution of SWCNTs produced by C_2H_2 may have the similar cause as that produced by CH_4, in which a reducing agent (H_2) is the byproduct of C_2H_2 decomposition. However, for C_2H_5OH and CH_3OH, oxygen-containing species, like OH radicals, have been suggested to facilitate the oxidation of amorphous carbon.[26] OH radicals may also provide a balance of the C and H ratio to favor SWCNT growth, which leads to narrower (*n*,*m*) distribution. We have co-fed 1 sccm of H_2 for C_2H_5OH and CH_3OH growth; few SWCNTs were produced with H_2. We suspect that the difference between C_2H_5OH and CH_3OH may be due to the different C:H:O ratios (2:6:1 and

(23) Lu, C.; Liu, J. *J. Phys. Chem. B* **2006**, *110* (41), 20254−20257.

(24) Lolli, G.; Zhang, L.; Balzano, L.; Sakulchaicharoen, N.; Tan, Y.; Resasco, D. E. *J. Phys. Chem. B* **2006**, *110* (5), 2108−2115.

(25) Zhang, G.; Mann, D.; Zhang, L.; Javey, A.; Li, Y.; Yenilmez, E.; Wang, Q.; McVittie, J. P.; Nishi, Y.; Gibbons, J.; Dai, H. *Proc. Natl. Acad. Sci. U.S.A.* **2005**, *102* (45), 16141−16145.

(26) Maruyama, S.; Kojima, R.; Miyauchi, Y.; Chiashi, S.; Kohno, M. *Chem. Phys. Lett.* **2002**, *360* (3,4), 229−234.

1:4:1, respectively) or the difference between the C−C bond of C_2H_5OH and the single carbon atom of CH_3OH. Further studies on the mechanistic differences are needed to clarify these issues.

Conclusion

In summary, we reported the successful synthesis of SWCNTs using four different carbon precursors on Co−Mo catalysts. Semiconducting (*n*,*m*) abundance was evaluated by a method based on a single-particle tight-binding theoretical model using photoluminescence and absorption microscopy. Narrowly (*n*,*m*) distributed SWCNTs can be obtained under high-pressure CO or vacuumed C_2H_5OH and CH_3OH predominately in the same higher chiral-angle region (*n*,*m*). For SWCNTs produced by diluted C_2H_2, reconstruction failure of E^S_{11} NIR absorption spectra suggests that photoluminescence spectra may miss tube fractions with larger diameters and smaller chiral angles. Carbon precursor pressure was found to be a key factor to the chirality control in this study. The carbon precursor chemistry may also play an important role in obtaining narrowly (*n*,*m*) distributed SWCNTs. The (*n*,*m*) selectivity on Co−Mo catalysts can be shifted by different carbon precursors.

Acknowledgment. This project is supported by the Nanyang Technological University CoE-SUG and AcRF Grant RG38/06. The authors thank reviewers for helpful comments.

Supporting Information Available: Tabulated values of the relative photoluminescence intensities for SWCNT samples, calculated PL intensities from the electron−phonon interaction model, and (*n*,*m*) abundance for samples; photoluminescence excitation intensity maps of three parallel runs for each carbon precursor; Comparison of PL spectra of SWCNTs produced by CO in different surfactants including single strain DNA, DOC, and SDS; experimental and reconstruction of E^S_{11} optical absorption spectra of SWCNTs produced by four carbon sources using abundance determined by single-mode log-normal distribution line-shape fitting and PL analysis. This material is available free of charge via the Internet at http://pubs.acs.org.

JA070808K